

Near-UV Background in Photonic Based pi'n/pin Amorphous SiC Sensors

Manuela Vieira, Manuel Augusto Vieira, Vitor Silva,
Paula Louro,
CTS/UNINOVA
Monte de Caparica, Portugal
e-mail: mv@isel.ipl.pt

Manuela Vieira, Manuel Augusto Vieira, Isabel
Rodrigues, Vitor Silva, Paula Louro,
DEETC/ISEL
Lisbon, Portugal
e-mail: mv@isel.ipl.pt

Abstract— In this paper, we present a wavelength selector based on a monolithic multilayer pi'n/pin a-SiC:H optical filter that requires appropriate near-ultraviolet steady states optical switches to select the desired wavelengths in the visible-near infrared (VIS-NIR) ranges. Results show that the background intensity works as a selector in the infrared/visible regions, shifting the sensor sensitivity. Low intensities select the NIR range while high intensities select the visible part. Here, the optical gain is very high in the red range, decreases in the green range, and stays near one in the blue region decreasing strongly in the near-ultraviolet range. The transfer characteristics effects due to changes in steady state light intensity and wavelength backgrounds are presented. The relationship between the optical inputs and the output signal is established when a multiplexed signal is analysed. An optoelectronic model gives insight into the physics of the selector.

Keywords- Integrated optical filter, VIS-NIR communications, Photonics-based sensors, Optoelectronics

I. INTRODUCTION

Newly developed technologies for infrared telecommunication systems allowed the increase of capacity, distance and functionality, switching and control with the design of new reconfigurable logic active filter gates by “bridging the gaps” and combining the optical filters properties. Expanding far beyond traditional applications in optical interconnects at telecommunication wavelengths [1] [2], the SiC nanophotonic integrated circuit platform has recently proven its merits for working with visible range optical signals. To enhance the transmission capacity and the application flexibility of optical communication efforts have to be considered, namely the Wavelength Division Multiplexing based on tandem a-SiC:H light controlled filters, when different visible signals are encoded in the same optical transmission path [3] [4]. In this paper, the shift of the visible range to telecom band can be accomplished using the same wavelength selector but under near-ultraviolet optical bias, acting as reconfigurable active filters in the visible and near infrared ranges. These active filters act as interface devices that establish the bridge between the infrared and red spectral range playing a key

role to bridging the infrared and the visible optical communication technology. They can be used to perform different filtering processes, such as: amplification, switching, and wavelength conversion.

After a short introduction, in Section II, the design, characterization, and operation of the device is described. In Section III, the light filtering properties are analyzed and in Section IV, the methodology that supports the visible/infrared tuning is presented. In Section V, an optoelectronic model gives insight into the physics of the device and, finally in Section VI the main conclusions are presented.

II. DEVICE DESIGN, CHARACTERIZATION AND OPERATION

The selector is realized by using a double pi'n/pin a-SiC:H photodetector with TCO front and back biased optical gating elements as depicted in Figure 1. The active device consists of a p-i'(a-SiC:H)-n/p-i(a-Si:H)-n heterostructure. The thicknesses and optical gap of the front i'- (200 nm; 2.1 eV) and back i- (1000 nm; 1.8 eV) layers are optimized for light absorption in the blue and red ranges, respectively [5].

Optoelectronic characterization was performed through spectral response and transmittance measurements without and with steady state applied optical bias. The optical bias (ϕ ; background) was superimposed using near-ultraviolet Light Emitting Diodes (LEDs) (390 nm). Currents between 0.005 mA and 30 mA were used to drive the LEDs in order to change the light flux background.

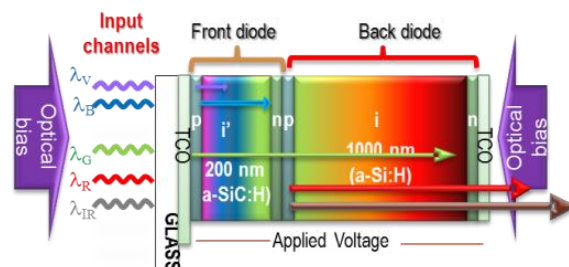


Figure 1. Device configuration and operation.

Monochromatic (infrared, red, green, blue and violet; $\lambda_{IR,R,G,B,V}$) pulsed communication channels (input channels) are combined together, each one with a specific bit sequence and absorbed accordingly their wavelengths (see arrow magnitudes in Figure 1). The combined optical signal (multiplexed signal; MUX) is analyzed by reading out the generated photocurrent under negative applied voltage (-8V), without and with near-ultraviolet background (390nm) and different intensities, applied either from front (λ_F) or back (λ_B) sides. The device operates within the visible/NIR range using as input color channels the square wave modulated low power light supplied by near-infrared/red (NIR/ R: 880 nm-626nm), green (G: 524 nm), blue (B: 470 nm) and violet (V: 400 nm) LEDs.

In Figure 2a, the transmittances from the front and back diodes are plotted as well as the transmittance of the complete device without any background light. In Figure 2b, the transmittance is displayed under different 390 nm background intensities.

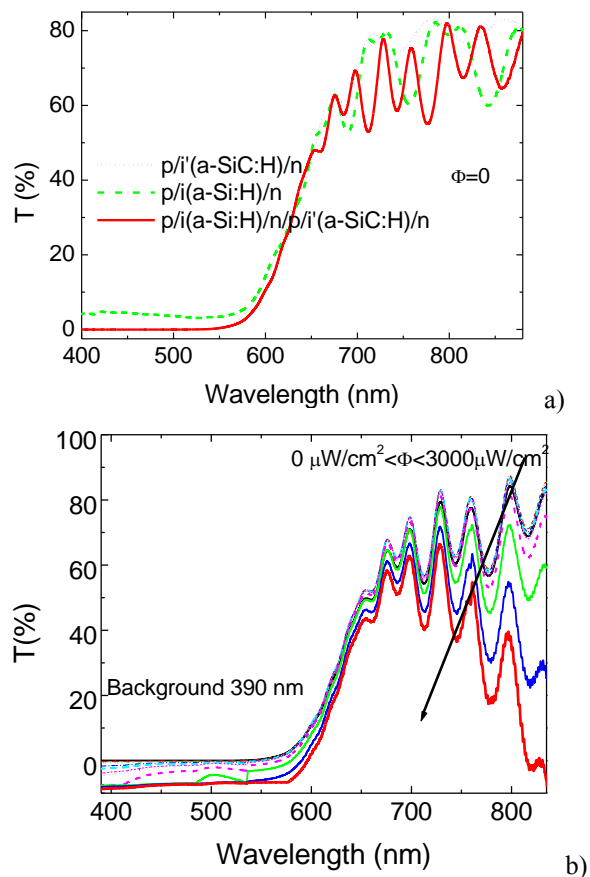


Figure 2. Transmittances from: a) front, back and whole device; b) the π -npin structure under front irradiation, with 390 nm irradiation and different intensities.

Results confirm the influence of the thickness of each front and back diode on the transmittance of the whole device. It is interesting to notice that under front light

irradiation, the transmittance decreases in the infrared range as the background intensity increases leading to an infrared absorption window.

III. LIGHT FILTERING PROPERTIES

The spectral sensitivity was tested through spectral response measurements [6] [7] without applied optical bias and under 390 nm front and back backgrounds of variable intensities. In Figure 3 the spectral gain (α), defined as the ratio between the spectral photocurrent with and without applied optical bias, is displayed under near-UV ($\lambda=390$ nm; Figures 3a and 3b) illuminations. In Figure 3a, the light was applied from the front (λ_F) and in Figure 3b, the irradiation occurs from the back side (λ_B). The background intensity (ϕ) was changed between $5 \mu W/cm^2$ and $3800 \mu W/cm^2$.

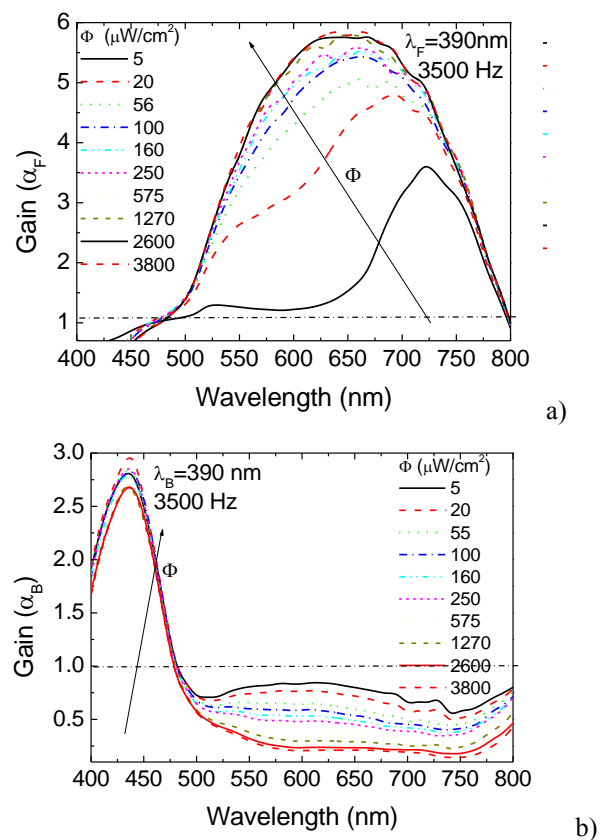


Figure 3. Front (a) and back (b) spectral gains ($\alpha_{F,B}$) under $\lambda=390$ nm irradiation.

Results show that the optical gains have opposite behaviors, under front and back irradiations. Under 390 nm front irradiation (Figure 3a) and low flux, the gain is high in the infrared region, presents a well-defined peak at 750 nm and strongly quenches the visible range. As the power intensity increases, the peak shifts to the visible range and can be deconvoluted into two peaks, one in the red range that slightly increases with the power density of the background and another in the green range that strongly

increases with the intensity of the ultra-violet radiation. In the blue range, the gain is much lower. This shows the controlled high-pass filtering properties of the device under different background intensities. Under back bias (Figure 3b) the gain in the blue/violet range has a maximum near 420 nm that quickly increases with the intensity. Besides it strongly lowers for wavelengths higher than 450 nm, acting as a short-pass filter. Thus, back irradiation, tunes the violet/blue region of the visible spectrum whatever the flux intensity, while front irradiation, depending on the background intensity, selects the infrared or the visible spectral ranges. Here, low fluxes select the near infrared region and cut the visible one, the reddish part of the spectrum is selected at medium fluxes, and high fluxes tune the red/green ranges with different gains.

IV. VISIBLE AND INFRA-RED TUNING

Four monochromatic pulsed lights separately (645nm, 697 nm, 850 nm and 880 nm input channels) or combined (MUX signal; Figure 5) illuminated the device at 12000 bps.

Steady state 390 nm bias at different intensities ($1\mu Wcm^{-2} < \phi_{F,B} < 3000\mu Wcm^{-2}$) were superimposed separately from the front and the back device side and the photocurrent was measured. The ratio between the photocurrent with and without applied optical bias was inferred and the gain for each wavelength channel determined. In Figure 4a, 880 nm transient signals at different flux irradiation are presented under front irradiations and back irradiations and in Figure 4b for the 645 nm channel the diverse gain are also displayed. In Figure 4c the gains for the four analyzed channels are shown as a function of the background intensity.

As expected from Figure 3, in the red/infrared spectral ranges, the optical gain depends on optical bias intensity and on the wavelength of the input channels. Results show that, even under transient conditions and using commercial visible and NIR LEDs, the background side and intensity alters the signal magnitude of the input channels. Under front irradiation, as the light flux increases, the magnitudes of all the input channels increases being higher at 645 nm then at 697 nm, 850 nm or 880 nm. Under back irradiation, as the flux intensity increases the magnitude of the channels decreases, quickly in the visible range and stays almost constant in the infrared range. Even across narrow bandwidths, the photocurrent gains are quite different (Figure 4c). This nonlinearity provides the possibility for selective tuning of the visible and IR wavelengths allowing their recognition.

In Figure 5, the MUX signals due to the combination of the four wavelength channels is displayed, under front and back irradiation. The signals were normalized to their values at the maximum flux.

Results confirm that the magnitude of the combined signal depends mainly on the channel wavelength through its own gain.

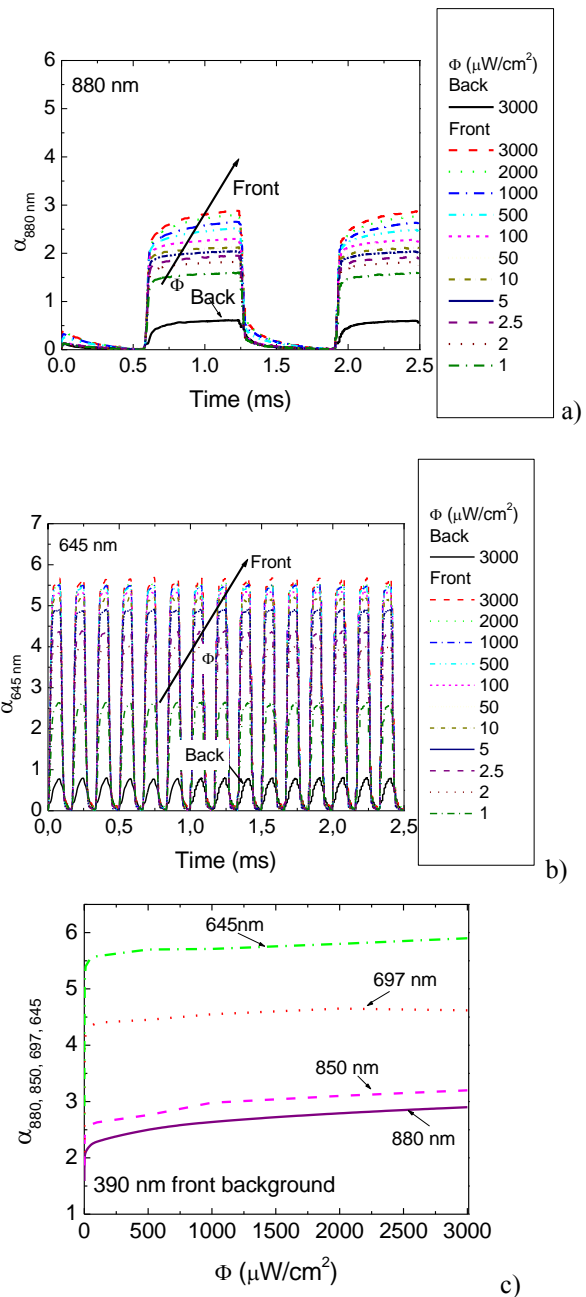


Figure 4. Front (a) and back (b) gains using $\lambda=390$ nm irradiation at different intensities. (c) Optical gains as a function of the background intensity.

Under front and back irradiation, the gains are different, front irradiation enhances the red/infrared channels (Figure 4c) while back light quench them. The gains inferred under $3000\mu W/cm^2$ back irradiation were respectively $\alpha_{880}=0.61$, $\alpha_{850}=1.03$, $\alpha_{697}=0.92$, $\alpha_{645}=0.85$.

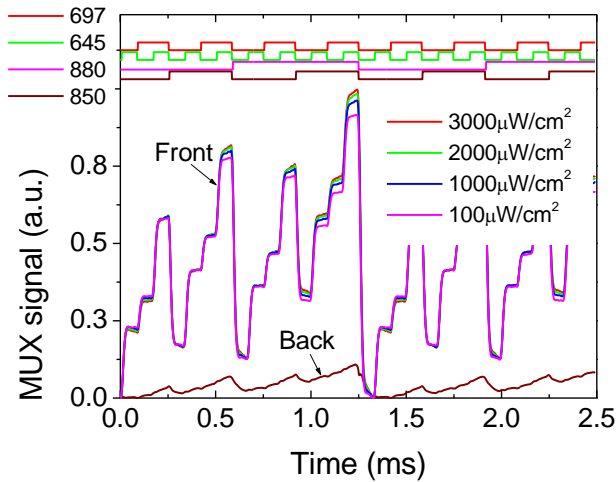


Figure 5. Front and back MUX signals under front and back $\lambda=390$ nm irradiation and different background intensities.

This nonlinearity allows identifying the different input channels in a narrow red/infrared range. The 390 nm radiation is absorbed at the beginning of the front diode and, due to the self-bias effect, increases the electric field at the back diode where the red/infrared incoming photons (see Figure 2) are absorbed accordingly to their wavelengths (see Figure 3) resulting in an increased collection. Under back irradiation, the electric field decreases mainly at the i-n back interface quenching the red/NIR input signals in different ways. This effect may be due to the increased absorption under back irradiation (Figure 2) that increases the number of carriers generated by the infra-red photons. So, by switching between front and back irradiation the photonic function is modified from a long- to a band-pass filter allowing, alternately selecting the red or the infrared channels, making the bridge between the visible and the infrared regions.

V. OPTOELECTRONIC MODEL

Based on the experimental results and device configuration a two connected phototransistors model (Figure 6a), made out of a short- and a long-pass filter was developed [5] and upgraded to include several input channels.

In Figure 6b, the block diagram of the optoelectronic state model is displayed. The resistors (R_1 , R_2) and capacitors (C_1 , C_2) synthesize the desired filter characteristics. The input signals, $\lambda_{IR,Rn,G,B,V}$ model the input channels and $i(t)$ the output signal. The amplifying elements, α_1 and α_2 are linear combinations of the optical gains of each impinging channel, respectively into the front and back phototransistors and take into account the enhancement or quenching of the channels (Figure 4) due to the steady state irradiation. Under front irradiation: $\alpha_2 \gg \alpha_1$ and under back irradiation $\alpha_1 \gg \alpha_2$. This affects the reverse

photo capacitances, $(\alpha_{1,2} / C_{1,2})$ that determine the influence of the system input on the state change.

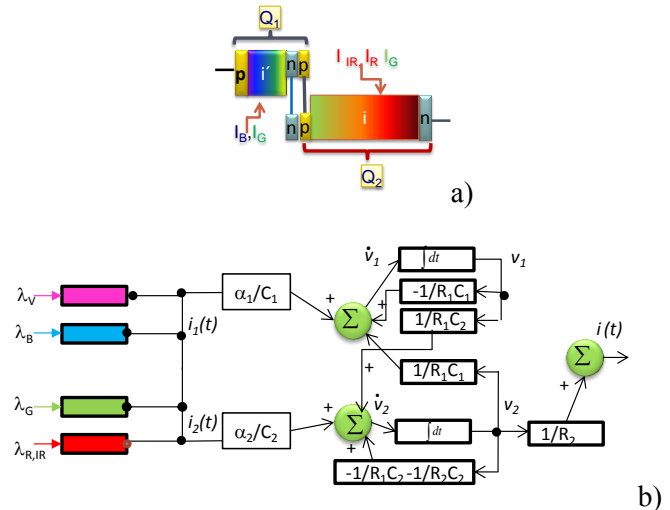
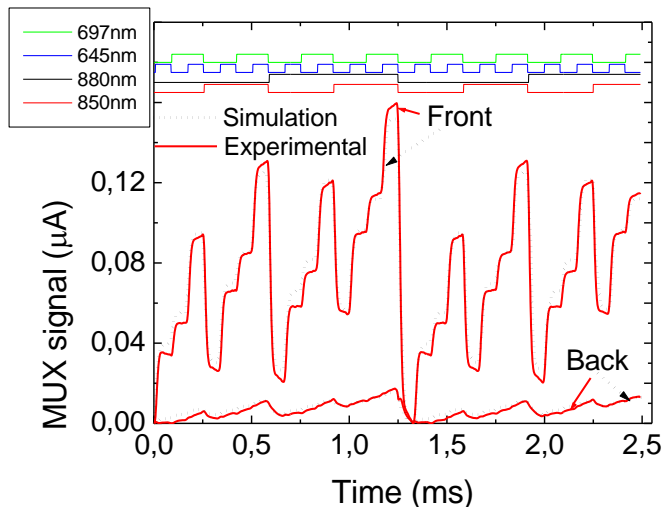


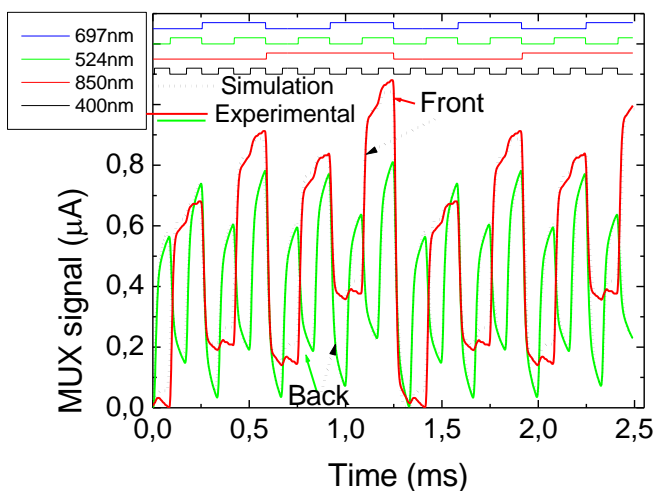
Figure 6. a) Two connected transistor model, b) block diagram of the optoelectronic state model.

A graphics user interface computer program was designed and programmed within the MATLAB® programming language, to ease the task of numerical simulation. This interface allows selecting model parameters, along with the plotting of both bit signal and simulated and experimental photocurrent results. To simulate the input channels we have used the individual magnitude of each input channel without background lighting, and the corresponding gain at the simulated background intensity (see Figures 4). Figure 7, presents results of a numerical simulation with $3000 \mu\text{W}/\text{cm}^2$ front and back $\lambda=390$ nm irradiation, using in Figure 7a the MUX signal of Figure 5 and in Figure 7b a VIS/NIR combination of $\lambda_V=400$ nm, $\lambda_G=524$ nm, $\lambda_R=697$ nm, $\lambda_{IR}=850$ nm input channels. Here, the front gains were $\alpha_V=0.82$, $\alpha_G=2.85$, $\alpha_R=4.35$, $\alpha_{IR}=3.27$ and the back ones, respectively: 11.5, 0.68, 0.92 and 0.5. Values of $R_1=10$ K Ω , $R_2=1$ K Ω , $C_1=1000$ pF, $C_2=20000$ pF were used during the simulation process (Figure 6b). On top of both figures the drive input LED signals guide the eyes into the different *on/off* states and correspondent wavelengths.

A good fitting between experimental and simulated results was achieved. The plots show the ability of the presented model to simulate the sensitivity behaviour of the proposed system in the visible/infrared spectral ranges. The optoelectronic model with light biasing control has proven to be a good tool to design optical filters. Furthermore, this model allows for extracting theoretical parameters by fitting the model to the measured data (internal resistors and capacitors).



a)



b)

Figure 7. Numerical simulation with front and back $\lambda=390$ nm irradiation, and different channel wavelength combinations

Under back irradiation higher values C_2 were obtained confirming the capacitive effect of the near-UV radiation on the device that increases the charge stored in the space charge layers of the back optical gate of Q_2 modelled by C_2 .

VI. CONCLUSIONS

An optoelectronic device based on a-SiC:H technology is analyzed. Tailoring the filter wavelength in the NIR/VIS was achieved by using near-ultraviolet backgrounds and changing the irradiation side and intensity. Results show that the pi'n/pin multilayered structure functions and parameters are reconfigurable under front and back irradiation, acting as data selector in the VIS/NIR ranges. The device performs wavelength division multiplexing (WDM) optoelectronic logic functions providing photonic functions such as signal amplification, filtering and

switching. The opto-electrical model with light biasing control has proven to be a good tool to design optical filters in the VIS/NIR. An optoelectronic model was presented and proven to be a good tool to design optical filters in the VIS/NIR range.

ACKNOWLEDGMENT

This work was supported by FCT (CTS multi annual funding) and PTDC/EEA-ELC/111854/2009 and PTDC/EEA-ELC/120539/2010.

REFERENCES

- [1] P. P. Yupapin and P. Chunpang, "An Experimental Investigation of the Optical Switching Characteristics Using Optical Sagnac Interferometer Incorporating One and Two Resonators," Optics & Laser Technology, Vol. 40, No. 2, 2008, pp. 273-277.
- [2] S. S. Djordjevic et al. "Fully Reconfigurable Silicon Photonic Lattice Filters With Four Cascaded Unit Cells" IEEE photonics Technology Letters, 23, NO. 1, january 1, 2011, pp.41-44.
- [3] M. Vieira, P. Louro, M. Fernandes, M. A. Vieira, A. Fantoni and J. Costa, "Three Transducers Embedded into One Single SiC Photodetector: LSP Direct Image Sensor, Optical Amplifier and Demux Device", Advances in Photodiodes", InTech, Chap.19, 2011, pp. 403-425.
- [4] M. A. Vieira, M. Vieira, J. Costa, P. Louro, M. Fernandes, and A. Fantoni, "Double pin Photodiodes with two Optical Gate Connections for Light Triggering: A capacitive two-phototransistor model", Sensors & Transducers Journal, 9, Special Issue, December 2010 , pp.96-120.
- [5] M.A. Vieira, P. Louro, M. Vieira, A. Fantoni, and A. Steiger-Garção, "Light-activated amplification in Si-C tandem devices: A capacitive active filter model" IEEE sensor journal, 12, NO. 6, 2012, pp. 1755-1762.
- [6] M. A. Vieira, M. Vieira, P. Louro, V. Silva, and A. S. Garção, "Photodetector with integrated optical thin film filters" Journal of Physics: Conference Series, 421, 012011 March 2013.
- [7] M. Vieira, M. A. Vieira, I. Rodrigues, V. Silva, and P. Louro, "Tuning optical a-SiC/a-Si active filters by UV bias light in the visible and infrared spectral ranges", Phys. Status Solidi, C, 2014, pp. 1-4 .Article first published online: 25 JUL 2014. DOI: 10.1002/pssc.201400020